

**EXPLICIT GUIDANCE EQUATIONS FOR MULTISTAGE
BOOST TRAJECTORIES**

By Fred Teren

**Lewis Research Center
Cleveland, Ohio**

NATIONAL AERONAUTICS AND SPACE ADMINISTRATION

**For sale by the Clearinghouse for Federal Scientific and Technical Information
Springfield, Virginia 22151 - Price \$2.00**

EXPLICIT GUIDANCE EQUATIONS FOR MULTISTAGE BOOST TRAJECTORIES

by Fred Teren

Lewis Research Center

SUMMARY

Explicit guidance equations are developed for steering multistage launch vehicles to injection conditions that satisfy typical lunar impact requirements. The calculus of variations is used to derive the required boundary conditions on the thrust direction at staging points. An approximate variational yaw steering law is also derived in order to minimize the payload loss in removing yaw velocity errors. The equations are programed for steering the Atlas-Centaur vehicle on the direct-ascent Surveyor mission. Results are presented that demonstrate targeting accuracy and payload capability (compared with optimized open-loop trajectories).

INTRODUCTION

An important factor in determining the success of a mission is the ability of the guidance laws to steer the vehicle during its propulsion phases so that vehicle constraints are not violated and the required burnout conditions are achieved. The guidance laws must be capable of steering the vehicle to its desired target over a wide range of flight conditions, called dispersions, which are caused mainly by deviations from nominal vehicle performance. In addition to the requirement for targeting accuracy, guidance equations should deliver near-maximum payload capability under nominal and dispersed flight conditions.

Many guidance laws have been used and discussed in the literature. Reference 1 contains a description of some of the most widely used formulations. With perturbation guidance schemes (e.g., ref. 2), the thrust direction is calculated from empirical functions of the state conditions (position, velocity, and acceleration). These functions, and the associated constants, are obtained from curve fits of a nominal and a volume of dispersed trajectories. The trajectories are flown with an optimized steering program (e.g., calculus of variations) and iterated to the required terminal conditions (a process known as preflight targeting). Required velocity equations have also been used, wherein

the thrust is pointed nearly parallel to the difference between the required and present velocity vectors. This method still requires empirical biasing functions to satisfy position constraints along the flight and to shape the trajectory to an optimum one. Again, pre-flight targeting is required to obtain the empirical functions and constants.

The explicit guidance equations used in this report differ from the perturbation and required velocity equations in that the steering laws are based on an approximate closed-form solution to the equations of motion, solved continuously during flight. Several advantages are inherent with this formulation:

(1) The equations are not tied to any nominal trajectory so that no retargeting is required when last-minute changes in vehicle or target parameters are introduced.

(2) The equations have great flexibility and can be used without change for a variety of missions and vehicles.

(3) The pitch and yaw steering laws closely approximate the form prescribed by the calculus of variations for maximum payload.

The pitch steering law used in this report was first introduced by MacPherson (ref. 3), whose results were later expanded by Cherry (ref. 4). In reference 3, explicit equations are developed for steering a single stage, with constant thrust and specific impulse, from any initial position and velocity to a prescribed orbit, expressed in terms of radius, velocity, and flight-path angle. This pitch steering law allows a closed-form solution for radius and radial velocity (as functions of time). The required thrust direction is calculated directly as a function of the present and desired terminal state and the time to cutoff (determined by the required velocity). An approximation is developed to estimate the time to cutoff. Reference 4 uses the same pitch steering law, but extends the results to include other possible burnout requirements. An explicit solution is also developed for engines that can be throttled.

In this report, equations are developed that allow the explicit guidance laws to steer an arbitrary number of stages, each operating at a constant thrust and specific impulse. The calculus of variations is used to determine the required boundary conditions at staging points. In addition, the variational method is used to develop an approximate optimum yaw steering law. A pseudotarget concept is introduced to compensate for Earth oblateness and other perturbing forces.

The explicit equations are applied to the three-stage direct-ascent Atlas-Centaur-Surveyor mission, where the final two stages are flown with guidance-generated (closed loop) steering commands. The booster stage is flown through the atmosphere with a pre-specified (open loop) steering program. The powered flight trajectory places the vehicle on a coast ellipse that results in lunar impact at the desired location with a prespecified time of flight. In addition, the perigee radius of the transfer ellipse is specified. Equations are developed that approximate these burnout requirements in terms of radius and radial velocity and thus allow the use of the closed-form solution obtained in reference 3.

The Surveyor mission has been chosen for study in this report because it represents an extremely difficult guidance problem. Among the mission and guidance requirements are

- (1) Closed-loop steering for two stages (sustainer and Centaur)
- (2) A velocity increment of approximately 27 000 feet per second added while steering closed loop
- (3) Variable launch azimuth and injection true anomaly, and the associated wide range of trajectory profiles
- (4) Accurate targeting to achieve lunar impact at the desired landing site with a pre-specified time of flight

The explicit equations have been programmed on an IBM 7094 computer along with two different vehicle and flight-environment simulations. A simplified program is used to obtain targeting and payload results, wherein ideal gravity and propulsion models are assumed. A detailed flight-simulation program is used to obtain dispersion results. The pseudotarget concept is used with this program to compensate for Earth oblateness and other perturbing forces. Targeting errors are expressed in terms of errors in injection perigee altitude, yaw velocity, and midcourse-correction requirements.

ANALYSIS

Explicit guidance equations are developed for steering the final two stages of a three-stage Atlas-Centaur launch vehicle to a set of injection conditions that result in a lunar impact at a prespecified landing site. The time of flight is also fixed in order to allow the Goldstone tracking station to view the lunar arrival. Because of atmospheric constraints, the booster stage is flown with an open-loop pitch program designed to minimize aerodynamic heating and loads. The upper stages (sustainer and Centaur) operate under near-vacuum conditions, and both of these stages are flown closed loop.

The following simplifying assumptions are used in the derivation of the guidance laws:

- (1) Spherical Earth, with an inverse-square force field
- (2) No atmospheric effects on upper stages
- (3) Constant-thrust specific-impulse operation for sustainer and Centaur stages
- (4) No perturbing bodies (in particular, a massless moon is assumed)

The effect of these assumptions will be considered later in the analysis, and the equations will be modified where required.

One stage is assumed in the initial derivation; the required continuity equations at staging points will be considered later in the analysis.

Pitch Steering Law

The steering laws are derived in a rotating radial, normal, circumferential coordinate system, defined by

$$\left. \begin{aligned} \hat{r} &= \frac{\vec{r}}{r} \\ \hat{h} &= \frac{\vec{r} \times \vec{v}}{|\vec{r} \times \vec{v}|} \\ \hat{\theta} &= \hat{h} \times \hat{r} \end{aligned} \right\} \quad (1)$$

(All symbols are defined in appendix A.) The assumptions stated earlier are used to write the differential equation for the radius

$$\ddot{r} + \frac{\mu}{r^2} - \omega^2 r = a(\hat{f} \cdot \hat{r}) \quad (2)$$

where

$$\left. \begin{aligned} a(t) &= \frac{a(0)}{1 - \frac{t}{\tau}} \\ \tau &= \frac{v_e}{a(0)} \\ v_e &= gI_{sp} \end{aligned} \right\} \quad (3)$$

and \hat{f} is the unit thrust direction. In equation (3) and in the development that follows, $t = 0$ refers to the present time along the trajectory, rather than any fixed value of time. The guidance law used for the radial component of thrust is (ref. 3)

$$\hat{f} \cdot \hat{r} = A + Bt + \frac{\frac{\mu}{r^2} - \omega^2 r}{a} \quad (4)$$

which is combined with equation (2) to give

$$\ddot{\mathbf{r}} = (\mathbf{A} + \mathbf{B}t)\mathbf{a} \quad (5)$$

Equation (5) can be integrated twice to give

$$\dot{\mathbf{r}}(\mathbf{T}) = \dot{\mathbf{r}}(0) + b_0\mathbf{A} + b_1\mathbf{B} \quad (6a)$$

$$\mathbf{r}(\mathbf{T}) = \mathbf{r}(0) + \dot{\mathbf{r}}(0)\mathbf{T} + c_0\mathbf{A} + c_1\mathbf{B} \quad (6b)$$

where

$$b_0 = \int_0^{\mathbf{T}} \mathbf{a}(t)dt = -v_e \log\left(1 - \frac{\mathbf{T}}{\tau}\right) = \Delta v \quad (7a)$$

$$b_n = \int_0^{\mathbf{T}} t^n \mathbf{a}(t)dt = b_{n-1}\tau - \frac{v_e \mathbf{T}^n}{n} \quad (7b)$$

$$c_0 = \int_0^{\mathbf{T}} \left[\int_0^t \mathbf{a}(s)ds \right] dt = b_0\mathbf{T} - b_1 \quad (7c)$$

$$c_n = \int_0^{\mathbf{T}} \left[\int_0^t s^n \mathbf{a}(s)ds \right] dt = c_{n-1}\tau - \frac{v_e \mathbf{T}^{n+1}}{n(n+1)} \quad (7d)$$

and s is a dummy variable of integration. If the value of \mathbf{T} (again, referenced to the present time) is known, equation (6) can be solved for values of \mathbf{A} and \mathbf{B} that will give the desired values of $\mathbf{r}(\mathbf{T})$ and $\dot{\mathbf{r}}(\mathbf{T})$ (provided that these values are consistent with vehicle capability). For the Surveyor mission, none of the variables \mathbf{T} , $\mathbf{r}(\mathbf{T})$, or $\dot{\mathbf{r}}(\mathbf{T})$ is explicitly specified. In order to make use of the closed-form solution, these variables must be specified in terms of the required Surveyor boundary conditions.

Surveyor Boundary Conditions

The (prespecified) translunar flight time essentially depends only on the injection energy, so that the injection energy must also be fixed. The shape of the transfer ellipse is then completely determined by the perigee radius. Maximum payload capability is ob-

tained by injecting at low altitudes (and perigee altitudes), which causes payload heating constraints to be violated. For this reason, the perigee radius has been fixed for Surveyor flights. The values of energy and perigee radius determine the eccentricity and semi-latus rectum of the translunar ellipse:

$$e = 1 + \frac{2Er_p}{\mu} \quad (8a)$$

$$p = \frac{\mu}{2E} (e^2 - 1) \quad (8b)$$

If the required true anomaly $\eta(T)$ were known, the values of r and \dot{r} at cutoff could be calculated from

$$r(T) = \frac{p}{1 + e \cos \eta(T)} \quad (9a)$$

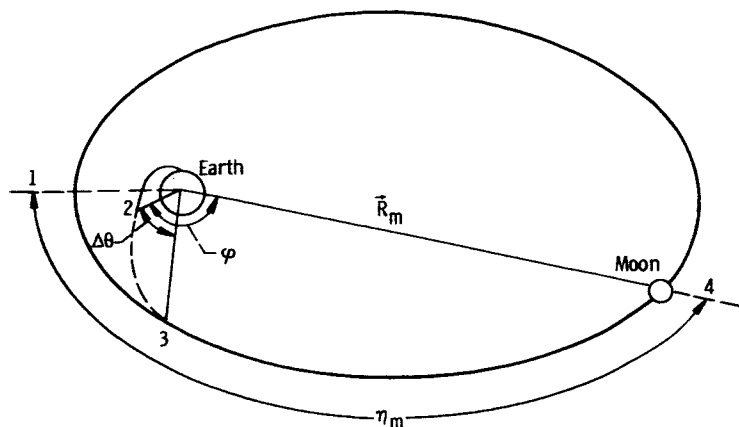
$$\dot{r}(T) = \sqrt{\frac{\mu}{p}} e \sin \eta(T) \quad (9b)$$

For Surveyor trajectories, cutoff occurs when the required energy level has been achieved. The required true anomaly is determined by the Earth-moon geometry at impact and the length of the boost arc from launch to injection. Since the cutoff time and the length of the boost arc are not precisely known during flight, the explicit guidance equations require estimates of T and $\eta(T)$ in order to determine $r(T)$, $\dot{r}(T)$, and the steering constants A and B (from eq. (5)). These estimates should be reasonably accurate early in flight and should converge rapidly near cutoff, so that accurate targeting can be achieved with no appreciable degradation in performance. The equations used to estimate T and $\eta(T)$ will be developed later in the analysis.

Yaw Steering Law

Assuming an inverse-square gravity field (as stated earlier) gives the required injection condition on yaw velocity as

$$\left(\hat{h} \cdot \hat{R}_m \right)_T = 0 \quad (10)$$



- \vec{R}_m target vector
- θ polar angle
- φ angle from present position to target
- η_m target true anomaly
- 1 perigee of translunar ellipse
- 2 present position
- 3 estimated burnout position
- 4 target (moon)

Figure 1 - Lunar transfer geometry.

where \hat{R}_m is a unit vector directed at the target, assumed fixed in space (see fig. 1). It is stated in equation (10) that the injection r, v plane contains the target vector. Differentiating equation (10) gives

$$\frac{d}{dt} (\hat{h} \cdot \hat{R}_m) = - \frac{a}{v_\theta} (\hat{f} \cdot \hat{h}) (\hat{\theta} \cdot \hat{R}_m) \quad (11)$$

where

$$v_\theta = \vec{v} \cdot \hat{\theta}$$

Equations (10) and (11) can be used to restate the requirement on yaw velocity:

$$\left(\hat{h} \cdot \hat{R}_m \right)_0 - \int_0^T \frac{a}{v_\theta} (\hat{f} \cdot \hat{h}) (\hat{\theta} \cdot \hat{R}_m) dt = 0 \quad (12)$$

A component of thrust must be supplied in the yaw direction to remove the initial yaw velocity. Moreover, the yaw steering program must be optimized so that the payload loss due to yaw steering is minimized. The appropriate yaw steering law is derived in appendix B by using an approximate calculus-of-variations solution:

$$\hat{f} \cdot \hat{h} = K \left(\frac{\hat{\theta} \cdot \hat{R}_m}{v_\theta} \right) \quad (13)$$

The gain constant K can be calculated by combining equations (12) and (13):

$$K = \frac{\left(\hat{h} \cdot \hat{R}_m \right)_0}{\int_0^t a \left(\frac{\hat{\theta} \cdot \hat{R}_m}{v_\theta} \right)^2 dt} \quad (14)$$

The integral in equation (14) cannot be explicitly determined during flight, so that an approximation is required to determine the gain constant K .

Yaw Integral Approximation

In order to evaluate the integral in equation (14), a linear variation is assumed for $(\hat{\theta} \cdot \hat{R}_m)/v_\theta$:

$$\frac{\hat{\theta} \cdot \hat{R}_m}{v_\theta} \sim d_1 + d_2 t \quad (15a)$$

where

$$d_1 = \left(\frac{\hat{\theta} \cdot \hat{R}_m}{v_\theta} \right)_0 \quad (15b)$$

$$d_2 = \frac{\left(\frac{\hat{\theta} \cdot \hat{R}_m}{v_\theta} \right)_T - d_1}{T} \quad (15c)$$

Equation (7) is now used to evaluate the yaw integral

$$\int_0^T a \left(\frac{\hat{\theta} \cdot \hat{R}_m}{v_\theta} \right)^2 dt = d_1^2 b_0 + 2d_1 d_2 b_1 + d_2^2 b_2 \quad (16)$$

which gives

$$K = \frac{(\hat{h} \cdot \hat{R}_m)_0}{(d_1^2 b_0 + 2d_1 d_2 b_1 + d_2^2 b_2)} \quad (17)$$

and

$$\hat{f} \cdot \hat{h} = \frac{(\hat{h} \cdot \hat{R}_m)(\hat{\theta} \cdot \hat{R}_m)}{v_\theta (d_1^2 b_0 + 2d_1 d_2 b_1 + d_2^2 b_2)} \quad (18)$$

Estimate of Required True Anomaly

The differential equation for polar angle can be written

$$\ddot{\theta} = \frac{a}{r} (\hat{f} \cdot \hat{\theta}) - \frac{2h\dot{r}}{r^3} \quad (19)$$

which is integrated twice to give

$$\Delta\theta = \theta(T) - \theta(0) = \left(\frac{h}{r^2}\right)_0^T + \int_0^T \left[\int_0^t \frac{a}{r} (\hat{f} \cdot \hat{\theta}) ds \right] dt - 2 \int_0^T \left(\int_0^t \frac{h\dot{r}}{r^3} ds \right) dt \quad (20)$$

Since the variables $\hat{f} \cdot \hat{\theta}$ and h are not known explicitly as functions of time, several approximations are required in order to evaluate the integrals in equation (20). The thrust vector is directed close to the local horizontal in order to increase energy and angular momentum. Thus, the components of thrust along the radial and normal directions are relatively small so that the approximation

$$\hat{f} \cdot \hat{\theta} = \sqrt{1 - (\hat{f} \cdot \hat{r})^2 - (\hat{f} \cdot \hat{h})^2} \sim 1 - \frac{(\hat{f} \cdot \hat{r})^2}{2} - \frac{(\hat{f} \cdot \hat{h})^2}{2} \quad (21)$$

may be used. In addition, $\hat{f} \cdot \hat{r}$ and $\hat{f} \cdot \hat{h}$ (from eqs. (4) and (18)) can be assumed linear in time:

$$\hat{f} \cdot \hat{r} \sim f_{r0} + \dot{f}_r t \quad (22a)$$

$$f_{r0} = A + \left(\frac{\frac{\mu}{r^2} - \omega^2 r}{a} \right)_0 \quad (22b)$$

$$\dot{f}_r = B + \frac{\left(\frac{\frac{\mu}{r^2} - \omega^2 r}{a} \right)_T - f_{r0}}{T} \quad (22c)$$

and

$$\hat{f} \cdot \hat{h} \sim f_h + \dot{f}_h t \quad (23a)$$

$$f_h = \frac{(\hat{h} \cdot \hat{R}_m) d_1}{(d_1^2 b_0 + 2d_1 d_2 b_1 + d_2^2 b_2)} \quad (23b)$$

$$\dot{f}_h = \frac{d_2}{d_1} f_h \quad (23c)$$

Using these approximations gives $\hat{f} \cdot \hat{\theta}$ in the form

$$\hat{f} \cdot \hat{\theta} = f_\theta + \dot{f}_\theta t + \ddot{f}_\theta t^2 \quad (24)$$

where

$$f_\theta = 1 - \frac{\dot{f}_r^2}{2} - \frac{\dot{f}_h^2}{2} \quad (25a)$$

$$\dot{f}_\theta = -(\dot{f}_r \dot{f}_r + \dot{f}_h \dot{f}_h) \quad (25b)$$

$$\ddot{f}_\theta = -\frac{\ddot{f}_r^2 + \ddot{f}_h^2}{2} \quad (25c)$$

The radius varies only a few percent during the flight, so that r may be assumed constant in the first integral in equation (20):

$$r \sim \bar{r} = \frac{r(0) + r(T)}{2} \quad (26)$$

The expression $2\dot{h}r/r^3$ is the Coriolis acceleration, which is small compared with the thrust acceleration. A linear variation is therefore adequate for this term:

$$\frac{\dot{h}r}{r^3} \sim d_3 + d_4 t \quad (27)$$

where, as previously,

$$d_3 = \left(\frac{h\dot{r}}{r^3} \right)_0 \quad (28a)$$

$$d_4 = \frac{\left(\frac{h\dot{r}}{r^3} \right)_T - d_3}{T} \quad (28b)$$

The preceding approximations and equation (7) are used in the integration of equation (20) to give

$$\Delta\theta = \left(\frac{h}{r^2} \right)_0 T + \frac{1}{r} (f_\theta c_0 + \dot{f}_\theta c_1 + \ddot{f}_\theta c_2) - d_3 T^2 - \frac{d_4 T^3}{3} \quad (29)$$

Equation (29) leads to an estimate of the required true anomaly. From figure 1

$$\eta(T) = \eta_m + \Delta\theta - \theta \quad (30)$$

where η_m is the target vector true anomaly.

Estimate of Cutoff Time

The required angular momentum at cutoff is given by

$$h(T) = \sqrt{\mu p} \quad (31)$$

and the time derivative of angular momentum is

$$\dot{h} = ar(\hat{f} \cdot \hat{\theta}) \quad (32)$$

The required change in angular momentum is

$$\Delta h = h(T) - h(0) = \int_0^T ar(\hat{f} \cdot \hat{\theta}) dt \quad (33)$$

The approximations for $\hat{f} \cdot \hat{\theta}$ and r from equations (24) and (26) are used to give equation (33) in the form

$$\Delta h = \bar{r}(f_{\theta} b_0 + \dot{f}_{\theta} b_1 + \ddot{f}_{\theta} b_2) \quad (34)$$

Equation (34) can be expressed in terms of ideal Δv by expanding b . Using equation (7) yields

$$\Delta h = \bar{r} \left[(f_{\theta} + \dot{f}_{\theta} \tau + \ddot{f}_{\theta} \tau^2) \Delta v - v_e T (\dot{f}_{\theta} + \ddot{f}_{\theta} \tau) - \frac{\ddot{f}_{\theta} v_e T^2}{2} \right] \quad (35)$$

or

$$\Delta v = \frac{\left[\frac{\Delta h}{\bar{r}} + v_e T (\dot{f}_{\theta} + \ddot{f}_{\theta} \tau) + \frac{\ddot{f}_{\theta} v_e T^2}{2} \right]}{f_{\theta} + \dot{f}_{\theta} \tau + \ddot{f}_{\theta} \tau^2} \quad (36)$$

The terms containing T in equation (36) are small compared with $\Delta h/\bar{r}$ so that the updated estimate of T from the previous computer cycle can be used in evaluating Δv .

The new estimate of T is obtained by combining equations (7a) and (36):

$$\Delta v = -v_e \log \left(1 - \frac{T}{\tau} \right) \quad (37a)$$

$$T = \tau \left(1 - e^{-\Delta v/v_e} \right) \quad (37b)$$

Extension to Two Stages

The calculus of variations shows (ref. 5) that the thrust direction and rate \hat{f} and $\hat{\dot{f}}$ should be continuous across staging for optimum performance. Since the acceleration will be discontinuous at staging points, A and B must also be discontinuous in order to satisfy the continuity of \hat{f} and $\hat{\dot{f}}$. Differentiating equation (4) results in

$$\frac{d}{dt} (\hat{f} \cdot \hat{r}) = B - \frac{\frac{\mu}{r^2} - \omega^2 r}{v_e} + \frac{\left(3\omega^2 - \frac{2\mu}{r^3}\right) \dot{r}}{a} - 2\omega(\hat{f} \cdot \hat{\theta}) \quad (38)$$

so that the required continuity equations are

$$A_1 + B_1 T_1 + \frac{\left(\frac{\mu}{r^2} - \omega^2 r\right)_s}{a_1(T_1)} = A_2 + \frac{\left(\frac{\mu}{r^2} - \omega^2 r\right)_s}{a_2(0)} \quad (39a)$$

$$B_1 - \frac{\left(\frac{\mu}{r^2} - \omega^2 r\right)_s}{v_{e,1}} + \frac{\left[\left(3\omega^2 - \frac{2\mu}{r^3}\right) \dot{r}\right]_s}{a_1(T_1)} - 2\omega(\hat{f} \cdot \hat{\theta})$$

$$= B_2 - \frac{\left(\frac{\mu}{r^2} - \omega^2 r\right)_s}{v_{e,2}} + \frac{\left[\left(3\omega^2 - \frac{2\mu}{r^3}\right) \dot{r}\right]_s}{a_2(0)} - 2\omega(\hat{f} \cdot \hat{\theta}) \quad (39b)$$

and the discontinuities in A and B are

$$\Delta A = A_2 - A_1 - B_1 T_1 = \left(\frac{\mu}{r^2} - \omega^2 r\right)_s \left[\frac{1}{a_1(T_1)} - \frac{1}{a_2(0)} \right] \quad (40a)$$

$$\Delta B = B_2 - B_1 = -\left(\frac{\mu}{r^2} - \omega^2 r\right)_s \left(\frac{1}{v_{e,1}} - \frac{1}{v_{e,2}} \right) + \left[\left(3\omega^2 - \frac{2\mu}{r^3}\right) \dot{r} \right]_s \left[\frac{1}{a_1(T_1)} - \frac{1}{a_2(0)} \right] \quad (40b)$$

The additional subscripts 1 and 2 introduced in equations (39) and (40) refer to the sustainer and Centaur stages, and the subscript s refers to conditions at staging. The time reference point for the Centaur stage is set at Centaur startup (during sustainer phase).

For two stages, equation (6) becomes

$$\dot{r}(T) = \dot{r}(0) + (b_{0,1} + b_{0,2})A_1 + (b_{1,1} + b_{1,2} + b_{0,2}T_1)B_1 + b_{0,2} \Delta A + b_{1,2} \Delta B \quad (41a)$$

$$r(T) = r(0) + \dot{r}(0)(T_1 + T_2) + (c_{0,1} + c_{0,2} + b_{0,1}T_2)A_1 \\ + (c_{1,1} + b_{1,1}T_2 + c_{0,2}T_1 + c_{1,2})B_1 + c_{0,2} \Delta A + c_{1,2} \Delta B \quad (41b)$$

In order to determine ΔA and ΔB from equation (40), estimates of position and velocity at sustainer cutoff are required. These estimates are obtained by using equations (6) and (34).

$$\dot{r}(T_1) = \dot{r}(0) + b_{0,1}A_1 + b_{1,1}B_1 \quad (42a)$$

$$r(T_1) = r(0) + \dot{r}(0)T_1 + c_{0,1}A_1 + c_{1,1}B_1 \quad (42b)$$

$$h(T_1) = \frac{[r(0) + r(T_1)]}{2} (\dot{f}_{\theta,1}b_{0,1} + \dot{f}_{\theta,1}b_{1,1} + \ddot{f}_{\theta,1}b_{2,1}) \quad (42c)$$

$$v_{\theta}(T_1) = \frac{h(T_1)}{r(T_1)} \quad (42d)$$

Boundary Condition on Yaw Thrust Direction

The calculus of variations requires the yaw thrust direction to be continuous across staging, which implies that K in equation (13) is continuous. However, the derivative of $\hat{f} \cdot \hat{h}$ is not continuous, since the derivative of \hat{h} involves acceleration (and is consequently discontinuous). Thus, different values of d_1 and d_2 are required for each stage.

Extension of Estimates to Two Stages

Yaw integral. - For two stages, equation (16) becomes

$$\int_0^T a \left(\frac{\hat{\theta} \cdot \hat{R}_m}{v_{\theta}} \right)^2 dt = \sum_{\ell=1}^2 (d_{1,\ell}^2 b_{0,\ell} + 2d_{1,\ell} d_{2,\ell} b_{1,\ell} + d_{2,\ell}^2 b_{2,\ell}) \quad (43)$$

Boost arc. - The estimate of $\Delta\theta$ for each stage is

$$\Delta\theta_{\ell} = \left(\frac{h}{r^2}\right)_{0,\ell} T_{\ell} + \frac{1}{r_{\ell}} (f_{\theta,\ell} c_{0,\ell} + \dot{f}_{\theta,\ell} c_{1,\ell} + \ddot{f}_{\theta,\ell} c_{2,\ell}) - d_{3,\ell} T_{\ell}^2 - \frac{d_{4,\ell}}{3} T_{\ell}^3 \quad (44)$$

and the total $\Delta\theta$ is

$$\Delta\theta = \Delta\theta_1 + \Delta\theta_2 \quad (45)$$

Cutoff time. - The sustainer stage cutoff time is assumed fixed, equal to its nominal value. Equation (42c) is used to estimate the angular momentum at Centaur startup, and equation (36) supplies the estimate of second stage Δv , with $\Delta h = h(T) - h(T_1)$. Equation (37) is then used to estimate the Centaur stage cutoff time.

The staging logic presented in the preceding section is, of course, not limited to two stages. Equations (38) to (45) are derived for an arbitrary number of stages (N) in appendix C.

Cutoff Logic

As cutoff energy is approached, the equations for calculating A, B, T, and K become indeterminate. If these calculations are continued up to cutoff, the values begin to oscillate and eventually diverge. For this reason, it is necessary to terminate the major calculation loop prior to cutoff and to steer the vehicle for the rest of the flight by using the last calculated values in equations (4) and (18). It is important, however, not to terminate these calculations too far from cutoff or targeting accuracy may be degraded because of errors in the last estimates of A and B. For Atlas-Centaur-Surveyor simulations, a value of "energy-to-go" corresponding approximately to 10 seconds prior to cutoff has been used with good results to terminate the major calculation loop.

Although the last estimates of A and B allow accurate targeting, the last estimate of cutoff time is not accurate enough to use for actual termination of powered flight. A more accurate method has been developed for this purpose in which energy is assumed to be a parabolic function of time. The coefficients of the energy-time polynomial are obtained by using the last three calculated time and energy values prior to cutoff. The cutoff time is determined by solving the quadratic.

EXTENSION TO REAL WORLD PROBLEM

The equations in the preceding sections have been derived by using several simplifying propulsion and gravity assumptions. Adjustments for these assumptions must be

made in two areas - navigational equations and steering equations. Both these areas will be considered in the following sections.

Propulsion Effects

The thrust and specific impulse of a real vehicle are not constant throughout flight, but the variations are usually small enough so that equation (3) can be used without degrading performance or accuracy. The measured acceleration and nominal specific impulse (for each stage) are used as inputs to the equations to estimate the future acceleration history. No in-flight measurement of specific impulse is assumed, because the noise in such measurements generally exceeds the expected (statistical) deviation from the nominal value. Simulations have shown that targeting accuracy is not degraded when large 3σ dispersions in specific impulse are introduced.

Atmospheric Effects

Atmospheric forces are large during booster phase, but this stage is flown open-loop so that the guidance equations are not affected. All contact forces are detected by the accelerometers so that navigational accuracy is also unaffected. Since atmospheric forces have greatly diminished at guidance closure, no special logic is needed in the steering equations to compensate for these effects. The guidance equations simply treat all measured forces as if they were a result of thrust.

Gravity Effects

In the preceding analysis, a spherical Earth and no perturbing bodies were assumed. The real Earth, however, is oblate and does not have a simple inverse-square gravity field. In addition, the translunar trajectory is perturbed by the moon, the sun, and the planets. Since the guidance accelerometers do not detect gravitational forces, a gravity model must be prestored on the guidance computer and used in the navigational equations.

One possibility is to store an oblate Earth gravity model, as well as ephemerides for the moon, the sun, and the planets, and thus determine the trajectory with great precision; however, this procedure is undesirable for several reasons. First, the free-flight equations of motion cannot be solved analytically when perturbing forces are present, so that the required injection conditions cannot be precisely determined. Second, storage limitations on most flight computers would preclude the possibility of storing such a

large amount of gravity data.

An alternate method that has been used with good results is the pseudotarget method, wherein a spherical gravity model is assumed for Earth and no perturbing forces are considered. An iteration is performed in the targeting process to determine the direction of the pseudotarget vector, as well as the pseudoenergy and perigee radius, which satisfy the real world injection and lunar impact requirements under nominal flight conditions. When dispersions are introduced, the trajectory profile varies somewhat, causing the compensated perturbing forces to have a slightly different effect on the trajectory. Targeting accuracy is somewhat degraded under these conditions; however, the magnitudes of the perturbing forces are small, so that their variation on perturbed flights is a minor effect, and targeting accuracy is not degraded significantly.

SURVEYOR MISSION

The direct-ascent Surveyor launch windows are characterized by the systematic variation of launch azimuth and injection true anomaly with time, as shown in figures 2 and 3. The variation of launch azimuth and true anomaly through any launch window is caused by the rotation of the Earth, while the particular curves to be followed in figures 2 and 3 are dictated mainly by the declination of the moon at arrival, as shown in the fig-

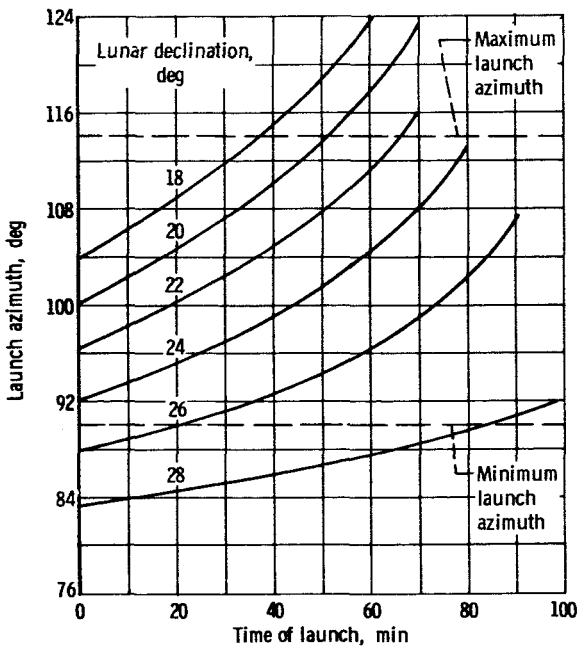


Figure 2 - Launch azimuth as function of time of launch.

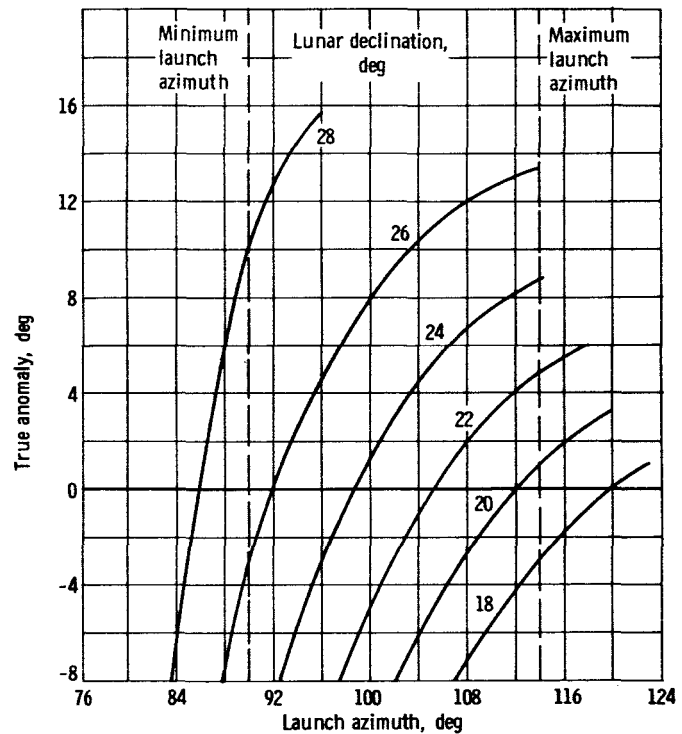


Figure 3 - True anomaly as function of launch azimuth.

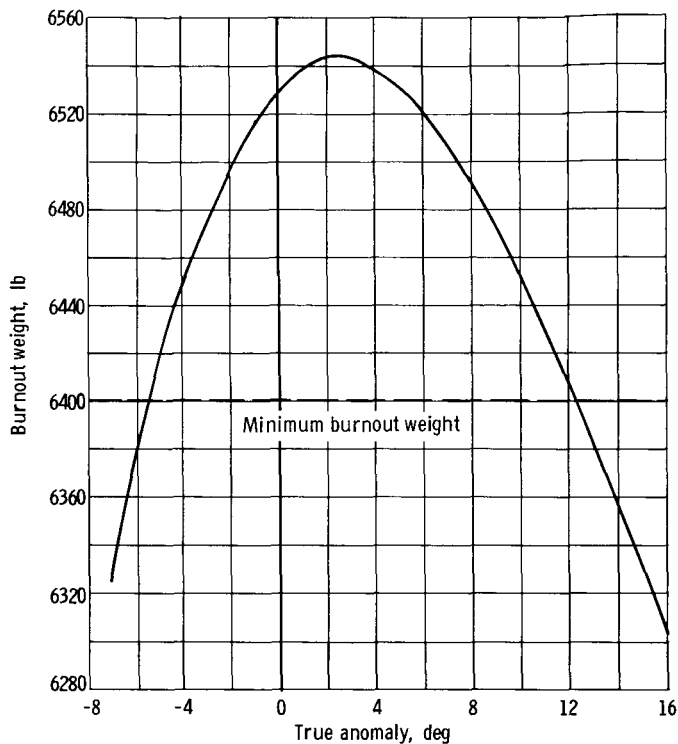


Figure 4. - Variation of burnout weight capability with injection true anomaly. Launch azimuth, 108 degrees.

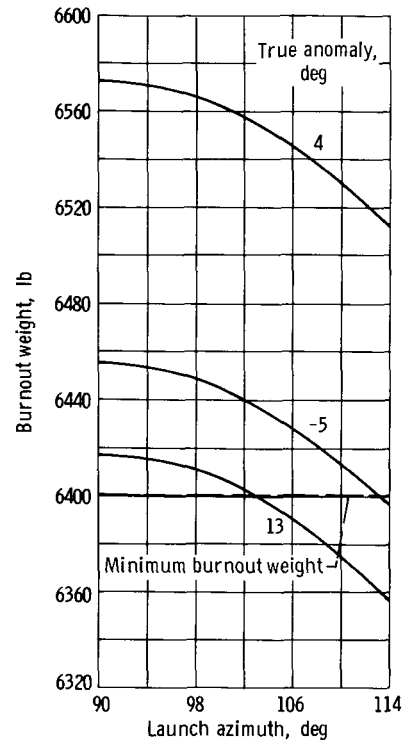


Figure 5. - Variation of burnout weight capability with launch azimuth for fixed true anomaly.

ures. The choice of zero time in the figures is arbitrary.

The duration of each launch window is determined by range safety launch azimuth limits, as indicated in figures 2 and 3, and by minimum allowable payload weight. The variation of payload capability with true anomaly and launch azimuth is shown in figures 4 and 5. The specification of a minimum payload weight limits the allowable true anomaly range, as shown in figure 4. The explicit guidance equations must be capable of steering the vehicle within the allowable range of launch azimuth and true anomaly.

VEHICLE DEFINITION

The Atlas-Centaur launch vehicle is sometimes referred to as a two and one-half stage vehicle because of the use of the sustainer engine during booster phase as well as during sustainer solo phase. In addition, the booster and sustainer engines share propellant tanks.

The vehicle lifts off with the booster and sustainer engines operating. At a predetermined acceleration level, the booster engines are shut down and jettisoned, while the propellant tanks are retained for use by the sustainer engine. Sustainer engine cutoff occurs at propellant depletion, at which time the sustainer engine and propellant tanks are

TABLE I. - VEHICLE AND FLIGHT ENVIRONMENT ASSUMPTIONS

Performance parameter	Simplified simulation			Detailed simulation		
	Booster	Sustainer	Centaur	Booster	Sustainer	Centaur
Thrust	$F_{sl} + A_{ex} \Delta P$	Constant	Constant	Detailed propulsion model		Constant
Weight flow	Constant	Constant	Constant			Constant
Atmospheric forces	Yes	No	No	Yes	Yes	No
Gravity forces	Spherical Earth, no perturbing bodies			Oblate Earth model, plus perturbing forces due to sun, moon, and Jupiter		
Steering	Zero angle of attack	Closed loop		Series of constant pitch rates	Closed loop	

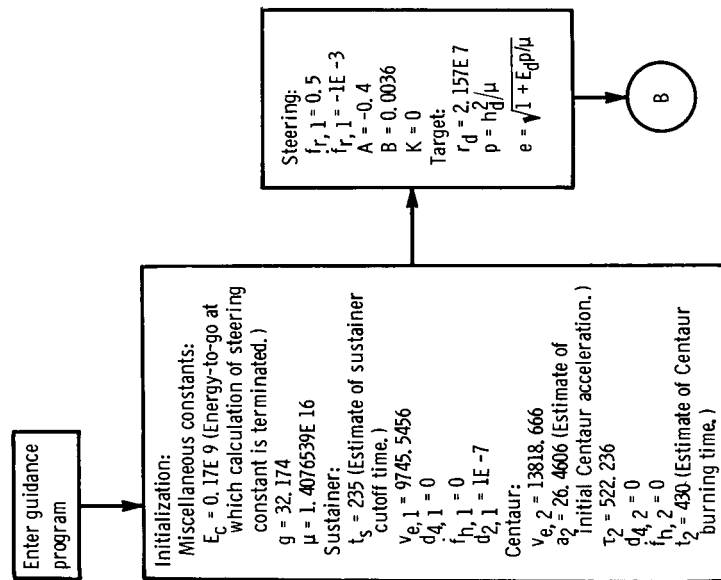
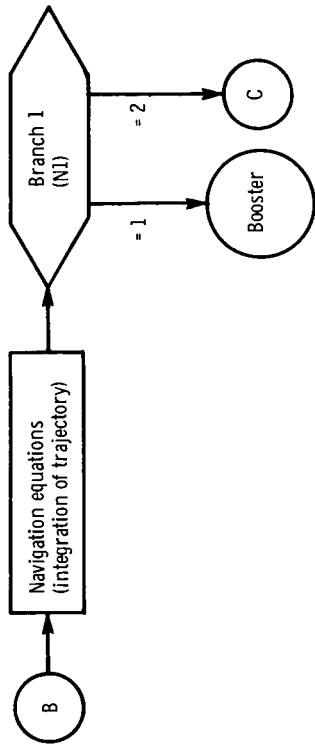
jettisoned. After a short delay, the Centaur engines ignite and burn until mission energy is achieved, at which time the Centaur engines are shut down.

Two different vehicle and flight environment simulations are used in the guidance equation simulation studies. The assumptions used with the two simulations are outlined in table I.

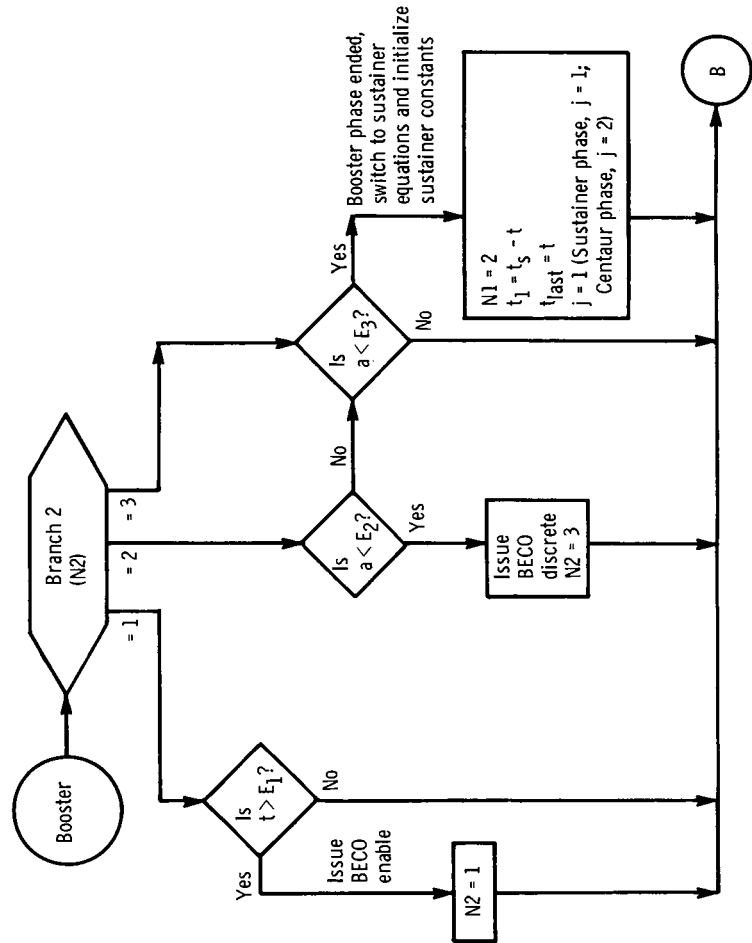
The detailed simulation uses a detailed propulsion model for the booster and sustainer engines. With this model, booster and sustainer thrust and weight flow are calculated as reference values plus linear perturbation terms that depend on atmospheric conditions, pump inlet conditions, acceleration, etc. The Centaur engine is assumed to operate at constant thrust and weight flow. A detailed atmosphere model is also used with this program, wherein aerodynamic lift and drag are considered and gimbaling of the booster and sustainer engines is used to cancel aerodynamic moments. The gravitational model includes a detailed oblate Earth and perturbing forces due to the sun, moon, and Jupiter in order to determine a precision translunar trajectory.

The simplified program uses only an exit-area - pressure correction term for booster thrust, while sustainer and Centaur thrust are assumed constant. All weight flows are assumed constant. The numerical values for this program are obtained from a "best fit" of the detailed trajectory.

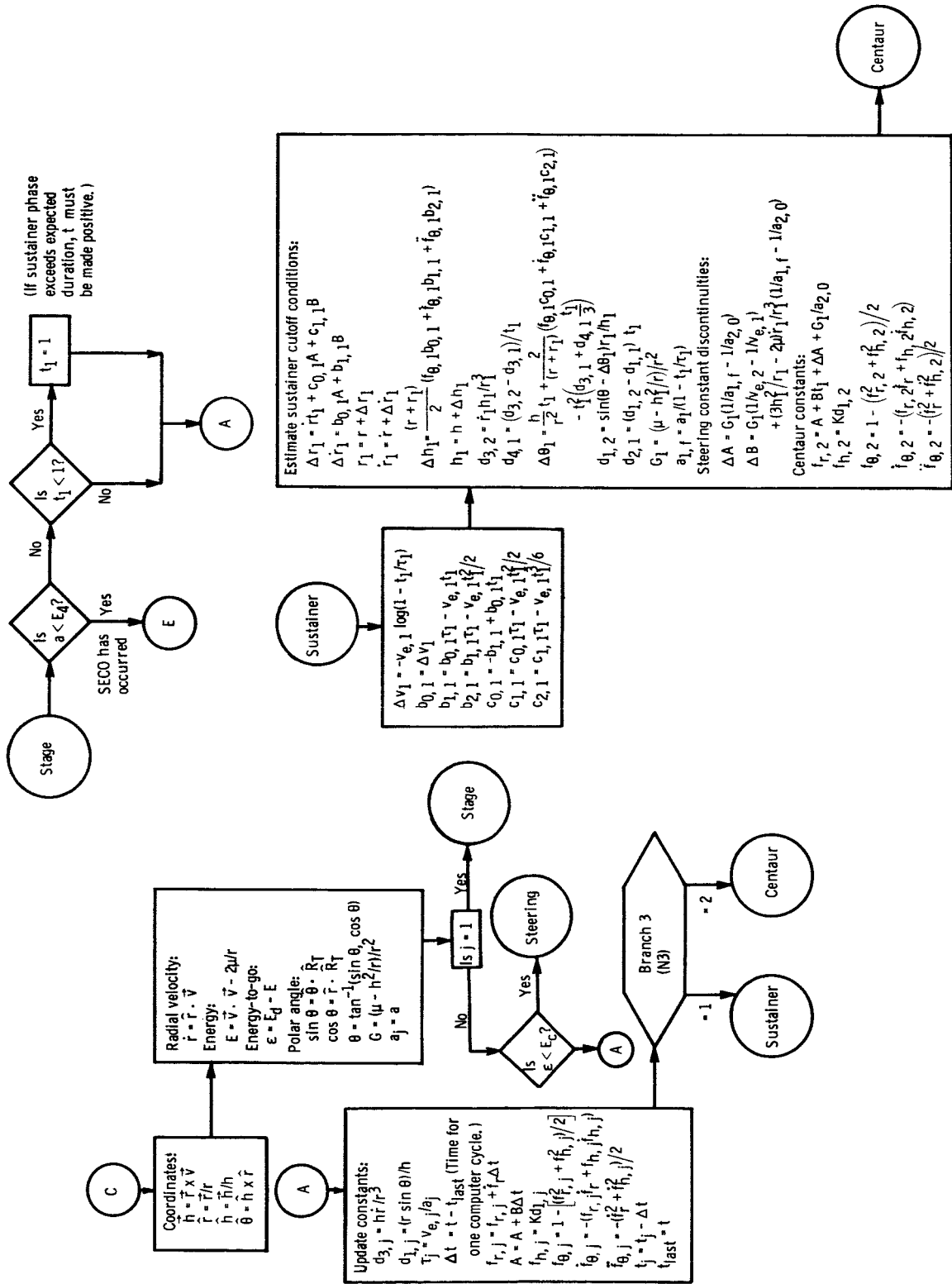
With the simplified program, the only atmospheric force considered is axial drag during boost phase. The Earth is assumed spherical, with an inverse-square force field, and no perturbing bodies are considered.



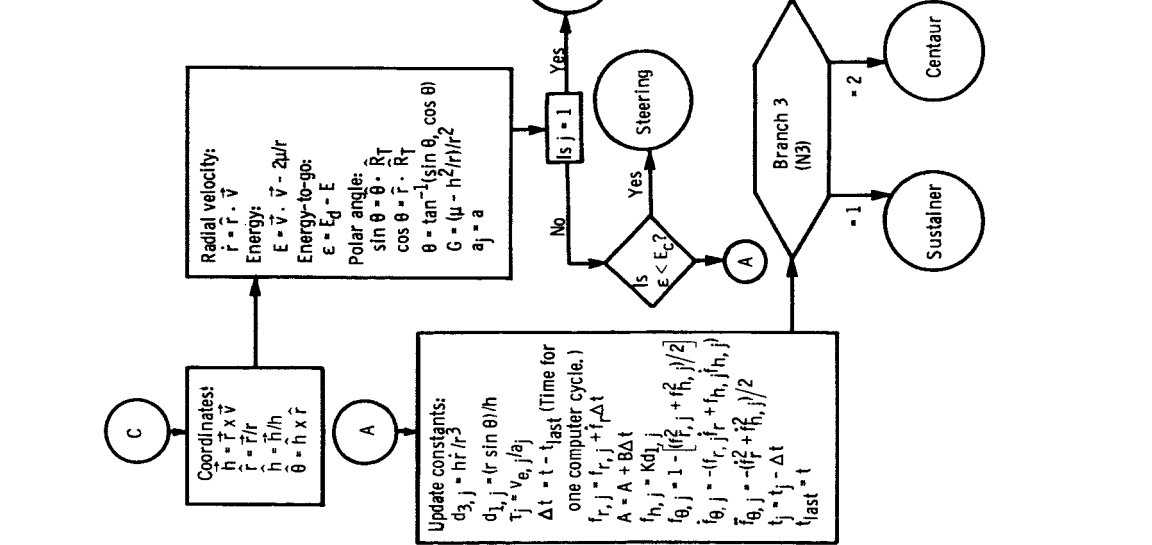
(a) Enter guidance program.



(b) Navigation and booster.

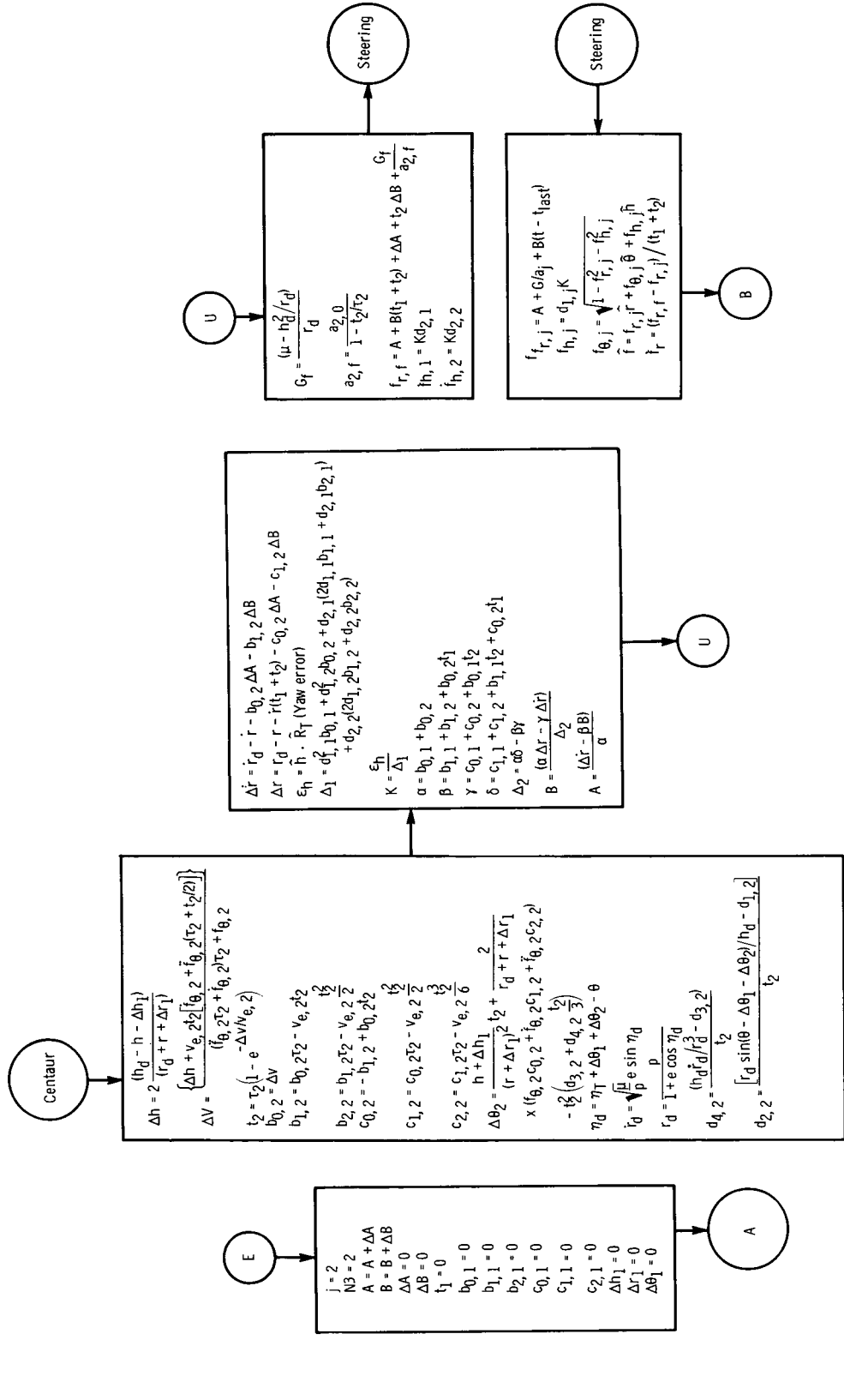


(d) Sustainer phase calculations.



(c) Coordinates and basic calculations for sustainer and Centaur.

Figure 6. - Explicit guidance equations flow charts.



(g) Steering and updating.

(f) Sustainer and Centaur phase calculations.

(e) Initialization for Centaur phase.

Figure 6. - Concluded.

The simulation of the explicit guidance equations used with both the simplified and detailed programs is outlined in figure 6. The flight computer navigational equations are not simulated; the real and guidance trajectories are both integrated using a fourth-order Runge-Kutta integration scheme. Flight computer navigational errors can be assumed small and are ignored here. All contact forces are used in the guidance-integrated trajectory, but a spherical Earth gravity model is used, consistent with the pseudotarget concept. Vehicle and computer time lags and response characteristics are not simulated.

RESULTS

The targeting accuracy and payload degradation of the explicit equations are demonstrated by using the simplified program. No targeting is required to compensate for gravity force with this program, since an ideal gravity model is used in the trajectory integration. The results obtained with this program are presented in table II.

The trajectories presented in table II cover the range of possible launch azimuth and true anomaly, as defined by figures 2 to 5. Targeting accuracy is evaluated in terms of errors in injection true anomaly, yaw velocity, and perigee radius. These errors are related to midcourse velocity requirements by approximate formulas derived in appendix D. Payload degradation is determined by comparison of guided trajectories with trajectories flown by using a calculus-of-variations steering program.

TABLE II. - TARGETING AND PAYLOAD RESULTS

Launch azimuth, deg	True anomaly, deg	Error in yaw velocity, ft/sec (a)	Error in perigee radius, ft (a)	Error in true anomaly, deg (a)	Payload loss, lb (b)	Midcourse correction requirements, ft/sec
92	15.4	-0.035	-146	0.00104	4.9	0.143
112	12.3	-.058	-125	.00087	4.3	.110
104	9.9	-.029	-104	.00053	4.3	.073
99	7.3	-.021	-90	-.00002	4.2	.007
96	4.6	-.013	-91	-.00005	4.2	.009
94	2.0	-.005	-89	-.00004	4.5	.006
92	-0.8	-.002	-89	-.00004	4.9	.006
91	-3.5	.003	-89	-.00096	5.4	.131
95	-6.4	0	-104	-.00048	7.4	.066

^aActual value minus desired value.

^bExplicit guidance equations minus calculus of variations.

TABLE III. - DISPERSION RESULTS (DETAILED PROGRAM)

Dispersion	Magnitude	Error in perigee radius, ft (a)	Change in weight, lb (a)	Midcourse correction requirement, ft/sec	
				Miss only (b)	Miss + time (c)
Booster specific impulse	-3.63 sec	-6	-81.4	0.197	0.550
Sustainer specific impulse	-3.07 sec	23	-51.3	.088	.148
Booster staging	-0.08 g	-26	3.1	.931	2.830
Booster pitch program	5 percent	-33	-18.2	.062	.370
Booster pitch program	-5 percent	21	-15.0	1.008	2.820
Centaur thrust	424 lb	35	-13.2	.288	1.188
Centaur specific impulse	-4.95 sec	67	-135.0	.206	.302
Centaur expendables	403 lb	-15	37.8	.655	1.781
Launch azimuth	2 deg	-30	-.6	1.399	5.260
Launch azimuth	-2 deg	27	-2.3	1.257	3.862
Root sum square	-----	96	171.5	2.108	6.770

^aDispersed minus nominal.

^bMidcourse ΔV to correct miss, allowing optimum time of flight.

^cMidcourse ΔV to correct miss and time of flight errors.

In order to demonstrate the validity of the pseudotarget concept, the detailed simulation program is used to target a trajectory under nominal conditions, and various dispersed trajectories are flown. These results are presented in table III.

The dispersions used in table III are statistical 3σ values. Although many other dispersions are possible, those presented in table III have the largest effect on injection conditions and midcourse velocity requirements, and the root-sum-square values obtained represent over 90 percent of the total obtained by using the complete dispersion list.

The results in table III show that perigee control is excellent in spite of the approximate gravity model used. The weight deviations are the result of performance losses associated with the dispersions, rather than degradation by the equations. The root-sum-square weight deviation represents the flight performance reserve required to compensate for 3σ performance dispersions.

Midcourse velocity requirements are calculated by using sensitivity coefficients, obtained by integrating the nominal trajectory and the adjoint equations to the moon on the detailed N-body program. Again, the root-sum-square values for miss only and miss plus time of flight indicate good performance.

Typical pitch and yaw steering profiles generated by using the explicit equations with the simplified trajectory program are presented in figures 7 and 8. The optimum calculus-of-variations profiles are also presented for comparison. The discontinuities

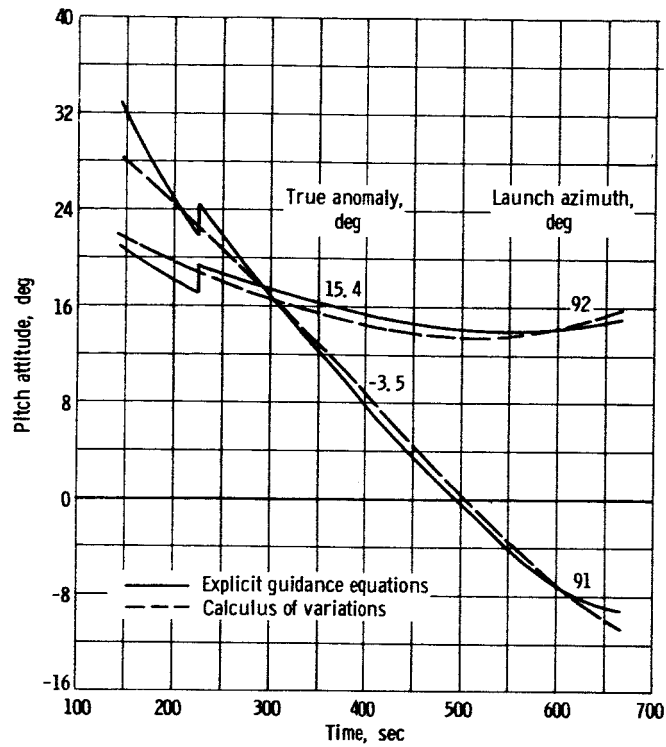


Figure 7. - Typical pitch profiles.

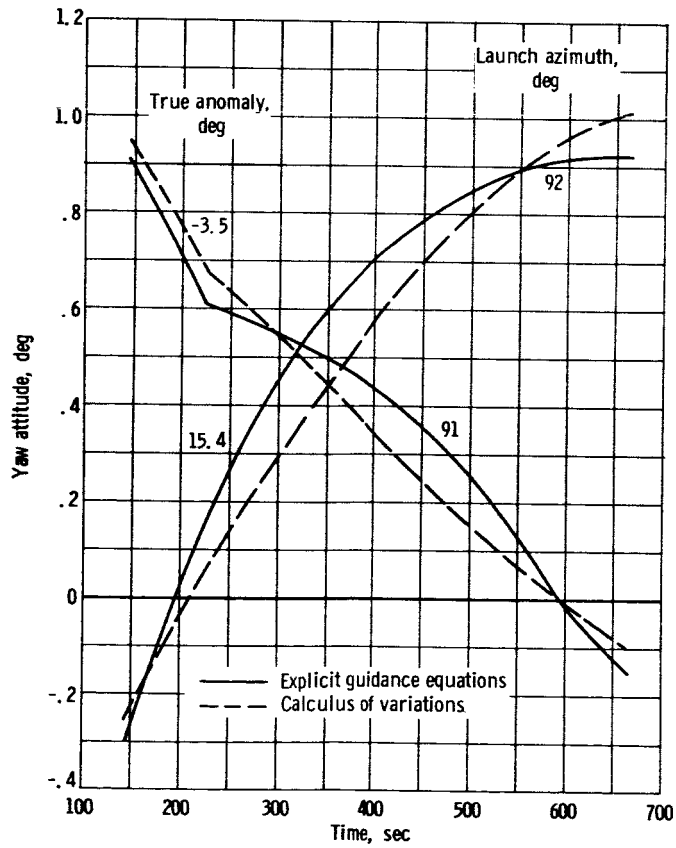


Figure 8. - Typical yaw profiles.

observed at sustainer cutoff are caused by errors in estimating sustainer cutoff conditions, and by the time lag before Centaur startup (ignored in the equations).

CONCLUDING REMARKS

Explicit guidance equations have been developed for steering a three-stage Atlas-Centaur boost vehicle to injection conditions that satisfy the Surveyor mission requirements. The targeting and dispersion results presented in tables II and III demonstrate the precision with which the explicit equations satisfy these requirements.

Before the equations can be implemented in a real vehicle, several additional study areas are required:

1. The explicit equations require more computer storage than the semiempirical velocity equations presently in use for the Surveyor mission. Preliminary estimates indicate that the explicit equations probably would not fit into the present Centaur computer, but would fit into several other existing and proposed flight computers.

2. Because of the large number of calculations required, cycle time could become excessively long, dependent, of course, on the computer speed. If this occurs, major and minor cycles could be introduced in which the latest steering constants are used to supply steering signals in the minor cycle (steering block, fig. 6(h)), while the steering constants are updated less frequently in the major cycle.

3. Some study is required to define (and, if necessary, to minimize) the coupling between the steering equations and the vehicle due to computer and autopilot time lags and response characteristics. These effects are related to the computer cycle time and should not present a problem because the minor cycle time can be made arbitrarily short.

In conclusion, the explicit equations presented appear to be an excellent choice for use with the direct-ascent Surveyor mission. The targeting and performance of the equations are excellent, and no severe problem areas appear to exist.

Because of the inherent accuracy and flexibility of the equations, their use can also be recommended for other lunar and planetary missions, both direct-ascent and parking orbit, as well as other less complex missions.

Lewis Research Center,
National Aeronautics and Space Administration,
Cleveland, Ohio, August 6, 1965.

APPENDIX A

SYMBOLS

A	steering constant (eq. (5)), nondimensional	K	yaw steering gain constant, ft/sec
A_{ex}	exit area, ft^2	M	target miss distance, ft
a	acceleration, ft/sec^2	m	mass, slugs
B	steering constant (eq. (5)), sec^{-1}	P	pressure, lb/ft^2
b, c	steering integrals (eq. (7))	p	semilatus rectum, ft
d	coefficient of linear polynomial (eqs. (15) and (28))	\hat{R}_m	unit target vector, nondimen- sional
E	energy per unit mass, ft^2/sec^2	r	radius, ft
E_c	energy-to-go at which steering constant calculations are terminated, ft^2/sec^2	r_m	target distance, ft
e	eccentricity, nondimensional	r_p	perigee radius, ft
F	thrust, lb	\bar{r}	average radius, ft
\hat{f}	unit thrust direction, nondimen- sional	$\hat{r}, \hat{\theta}, \hat{h}$	unit radial, circumferential, normal coordinate system, nondimensional
$f_x, \dot{f}_x, \ddot{f}_x$	x-components of unit accelera- tion direction ($x = r, \theta, h$)	T	cutoff time, sec
G	effective radial gravity accelera- tion, ft/sec^2	T_m	time of flight from midcourse to target, sec
g	Earth surface gravity accelera- tion, ft/sec^2	t	time, sec
h	angular momentum per unit mass, ft^2/sec	t_s	estimate of sustainer cutoff time, sec
I_{sp}	specific impulse, sec	v	velocity, ft/sec
J	functional to be minimized, $lb-sec^2/ft$	v_e	jet velocity, ft/sec
		v_h	yaw velocity, ft/sec
		Δv_L	velocity loss due to yaw steer- ing, ft/sec
		v_θ	circumferential velocity, ft/sec

α, β, γ	parameters used to calculate	d	desired
δ, Δ	steering constants (fig. 6)	f	final
ϵ	energy-to-go to cutoff, ft^2/sec^2	m	target
ϵ_h	yaw error, nondimensional	s	staging point
λ	Lagrange multiplier, $\text{lb}\cdot\text{sec}^2/\text{ft}$	s ℓ	sea level
μ	central body (Earth) force constant, ft^3/sec^2	T	cutoff
η	true anomaly, rad	0	present value
θ	polar angle, rad	1	sustainer phase
φ	angle from present position to target (fig. 1), rad	2	Centaur phase
τ	specific stage time, sec		Superscripts:
ω	angular velocity, rad/sec	($\dot{\quad}$)	derivative of ℓ, ℓ with respect to time
Subscripts:		\rightarrow	vector
c	midcourse	$\hat{\quad}$	unit vector

APPENDIX B

DERIVATION OF YAW STEERING LAW

The problem to be solved is to zero the initial yaw velocity error while minimizing the payload loss due to yaw steering. This payload loss is a result of a reduction in effective acceleration in the pitch plane. The amount of this reduction is

$$\Delta a = a \left[1 - \sqrt{1 - (\hat{f} \cdot \hat{h})^2} \right] \sim \frac{a}{2} (\hat{f} \cdot \hat{h})^2 \quad (\text{B1})$$

which gives a pitch plane velocity loss of

$$\Delta v_L = \int_0^T \frac{a}{2} (\hat{f} \cdot \hat{h})^2 dt \quad (\text{B2})$$

The velocity loss must be regained by expending additional propellants. Using equation (37a) results in

$$\Delta m_T = m_T \left(1 - e^{-\Delta v_L / v_e} \right) \sim \frac{m_T}{v_e} \Delta v_L \quad (\text{B3})$$

Equation (12) is used to state the problem mathematically as minimizing

$$\Delta m_T = \frac{m_T}{v_e} \int_0^T \frac{a}{2} (\hat{f} \cdot \hat{h})^2 dt \quad (\text{B4})$$

subject to the constraint

$$\int_0^T \frac{a}{v_\theta} (\hat{f} \cdot \hat{h})(\hat{\theta} \cdot \hat{R}_m) dt = (\hat{h} \cdot \hat{R}_m)_0 \quad (\text{B5})$$

This problem can be solved by using the calculus of variations and the method of undetermined Lagrange multipliers (ref. 6). Specifically,

$$J = \int_0^T \frac{m_T a}{2v_e} (\hat{f} \cdot \hat{h})^2 dt + \lambda \int_0^T \frac{a}{v_\theta} (\hat{f} \cdot \hat{h})(\hat{\theta} \cdot \hat{R}_m) dt \quad (B6)$$

where λ is an undetermined Lagrange multiplier. The payload loss is minimized when J is minimized and equation (B5) is satisfied. Taking the differential of J yields

$$\delta J = \int_0^T a \left[\frac{m_T}{v_e} (\hat{f} \cdot \hat{h}) + \lambda \frac{(\hat{\theta} \cdot \hat{R}_m)}{v_\theta} \right] \delta(\hat{f} \cdot \hat{h}) dt \quad (B7)$$

where a , $(\hat{\theta} \cdot \hat{R}_m)$, and v_θ have been assumed definite functions of time. To minimize J , it is required that $\delta J = 0$. Since the variation of $(\hat{f} \cdot \hat{h})$ is arbitrary, the term in brackets must be set equal to zero.

$$\hat{f} \cdot \hat{h} = K \left(\frac{\hat{\theta} \cdot \hat{R}_m}{v_\theta} \right) \quad (B8)$$

where

$$K = - \frac{v_e}{m_T} \lambda \quad (B9)$$

Equation (B8) is the yaw steering law to be used. The multiplier K is evaluated as in equation (14):

$$K = \frac{\hat{h} \cdot \hat{R}_T}{\int_0^T a \left(\frac{\hat{\theta} \cdot \hat{R}_m}{v_\theta} \right)^2 dt} \quad (B10)$$

APPENDIX C

DERIVATION OF N-STAGE CONTINUITY EQUATIONS

The discontinuities in A and B at each staging point are (following eq. (40))

$$\Delta A_j = A_{j+1} - A_j - B_j T_j = \left(\frac{\mu}{r^2} - \omega^2 r \right)_{s_j} \left(\frac{1}{a_j(T_j)} - \frac{1}{a_{j+1}(0)} \right) \quad (C1)$$

and

$$\Delta B_j = B_{j+1} - B_j = - \left(\frac{\mu}{r^2} - \omega^2 r \right)_{s_j} \left(\frac{1}{v_{e,j}} - \frac{1}{v_{e,j+1}} \right) + \left[\left(3\omega^2 - \frac{2\mu}{r^3} \right) \dot{r} \right]_{s_j} \left(\frac{1}{a_j(T_j)} - \frac{1}{a_{j+1}(0)} \right) \quad (C2)$$

and the steering constants for each stage are

$$B_j = B_1 + \sum_{\ell=1}^{j-1} \Delta B_\ell \quad (C3)$$

and

$$\begin{aligned} A_j &= A_1 + \sum_{\ell=1}^{j-1} (\Delta A_\ell + B_\ell T_\ell) \\ &= A_1 + \sum_{\ell=1}^{j-1} \left(\Delta A_\ell + B_1 T_\ell + T_\ell \sum_{k=1}^{\ell-1} \Delta B_k \right) \end{aligned} \quad (C4)$$

The change in \dot{r} for each stage is

$$\begin{aligned} \Delta \dot{r}_j &= b_{0,j} A_j + b_{1,j} B_j \\ &= b_{0,j} A_1 + \left(b_{1,j} + b_{0,j} \sum_{\ell=1}^{j-1} T_\ell \right) B_1 + \sum_{\ell=1}^{j-1} \left(b_{0,j} \Delta A_\ell + b_{0,j} T_\ell \sum_{k=1}^{\ell-1} \Delta B_k + b_{1,j} \Delta B_\ell \right) \end{aligned} \quad (C5)$$

and the initial \dot{r} for each stage is

$$\begin{aligned}
\dot{r}_j(0) &= \dot{r}_1(0) + \sum_{\ell=1}^{j-1} \Delta \dot{r}_\ell \\
&= \dot{r}_1(0) + \left(\sum_{\ell=1}^{j-1} b_{0,\ell} \right) A_1 + \left[\sum_{\ell=1}^{j-1} \left(b_{1,\ell} + b_{0,\ell} \sum_{k=1}^{\ell-1} T_k \right) \right] B_1 + \sum_{\ell=1}^{j-1} \sum_{k=1}^{\ell-1} \left(b_{0,\ell} \Delta A_k + b_{0,\ell} T_k \sum_{i=1}^{k-1} \Delta B_i \right. \\
&\quad \left. + b_{1,\ell} \Delta B_k \right) \tag{C6}
\end{aligned}$$

The change in r for each stage is

$$\begin{aligned}
\Delta r_j &= \dot{r}_j(0) T_j + c_{0,j} A_j + c_{1,j} B_j \\
&= \left(c_{0,j} + T_j \sum_{\ell=1}^{j-1} b_{0,\ell} \right) A_1 + \left[c_{1,j} + \sum_{\ell=1}^{j-1} \left(c_{0,j} T_\ell + b_{1,\ell} T_j + b_{0,\ell} T_j \sum_{k=1}^{\ell-1} T_k \right) \right] B_1 + \sum_{\ell=1}^{j-1} \left[c_{0,j} \Delta A_\ell \right. \\
&\quad \left. + c_{1,j} \Delta B_\ell + \sum_{k=1}^{\ell-1} \left(b_{0,\ell} T_j \Delta A_k + b_{0,\ell} T_k T_j \sum_{i=1}^{k-1} \Delta B_i + b_{1,\ell} T_j \Delta B_k + c_{0,j} T_\ell \Delta B_k \right) \right] + \dot{r}_1(0) T_j \tag{C7}
\end{aligned}$$

and the initial r for each stage is

$$\begin{aligned}
r_j(0) &= r_1(0) + \sum_{\ell=1}^{j-1} \Delta r_\ell \\
&= \sum_{\ell=1}^{j-1} \left(c_{0,\ell} + T_\ell \sum_{k=1}^{\ell-1} b_{0,k} \right) A_1 + \sum_{\ell=1}^{j-1} \left[c_{1,\ell} + \sum_{k=1}^{\ell-1} \left(c_{0,\ell} T_k + b_{1,k} T_\ell + b_{0,k} T_\ell \sum_{i=1}^{k-1} T_i \right) \right] B_1 \\
&\quad + \sum_{\ell=1}^{j-1} \sum_{k=1}^{\ell-1} \left[c_{0,\ell} \Delta A_k + c_{1,\ell} \Delta B_k + \sum_{i=1}^{k-1} \left(b_{0,k} T_\ell \Delta A_i + b_{0,k} T_i T_\ell \sum_{m=1}^{i-1} \Delta B_m \right. \right. \\
&\quad \left. \left. + b_{1,k} T_\ell \Delta B_i + c_{0,\ell} T_k \Delta B_i \right) \right] + \dot{r}_1(0) \sum_{\ell=1}^{j-1} T_\ell + r_1(0) \tag{C8}
\end{aligned}$$

The final r and \dot{r} are obtained from equations (C6) and (C8) by substituting $N+1$ for j :

$$\begin{aligned} \dot{r}(T) = \dot{r}_1(0) + \left(\sum_{\ell=1}^N b_{0,\ell} \right) A_1 + \left[\sum_{\ell=1}^N \left(b_{1,\ell} + b_{0,\ell} \sum_{k=1}^{\ell-1} T_k \right) \right] B_1 \\ + \sum_{\ell=1}^N \sum_{k=1}^{\ell-1} \left(b_{0,\ell} \Delta A_k + b_{0,\ell} T_k \sum_{i=1}^{k-1} \Delta B_i + b_{1,\ell} \Delta B_k \right) \end{aligned} \quad (C9)$$

$$\begin{aligned} r(T) = \sum_{\ell=1}^N \left(c_{0,\ell} + T_\ell \sum_{k=1}^{\ell-1} b_{0,k} \right) A_1 + \sum_{\ell=1}^N \left[c_{1,\ell} + \sum_{k=1}^{\ell-1} \left(c_{0,\ell} T_k + b_{1,k} T_\ell \right. \right. \\ \left. \left. + b_{0,k} T_\ell \sum_{i=1}^{k-1} T_i \right) \right] B_1 + \sum_{\ell=1}^N \sum_{k=1}^{\ell-1} \left[c_{0,\ell} \Delta A_k + c_{1,\ell} \Delta B_k + \sum_{i=1}^{k-1} \left(b_{0,k} T_\ell \Delta A_i \right. \right. \\ \left. \left. + b_{0,k} T_i T_\ell \sum_{m=1}^{i-1} \Delta B_m + b_{1,k} T_\ell \Delta B_i + c_{0,\ell} T_k \Delta B_i \right) \right] + \dot{r}_1(0) \sum_{\ell=1}^N T_\ell + r_1(0) \end{aligned} \quad (C10)$$

The estimates of staging conditions are obtained by using

$$\dot{r}(T_j) = \dot{r}_{j+1}(0) \quad (C11a)$$

$$r(T_j) = r_{j+1}(0) \quad (C11b)$$

$$h(T_j) = h_j(0) + \frac{[r_j(0) + r_{j+1}(0)]}{2} (f_{\theta,j} b_{0,j} + \dot{f}_{\theta,j} b_{1,j} + \ddot{f}_{\theta,j} b_{2,j}) \quad (C11c)$$

$$v_\theta(T_j) = \frac{h(T_j)}{r(T_j)} \quad (C11d)$$

The yaw integral in equation (43) becomes

$$\int_0^T a \left(\frac{\hat{\theta} \cdot \hat{R}_T}{v_\theta} \right)^2 dt = \sum_{\ell=1}^N \left(d_{1,\ell}^2 b_{0,\ell} + 2d_{1,\ell} d_{2,\ell} b_{1,\ell} + d_{2,\ell}^2 b_{2,\ell} \right) \quad (C12)$$

and the travel angle for each stage is

$$\Delta\theta_\ell = \left(\frac{h}{r^2}\right)_{0,\ell} T_\ell + \frac{1}{\bar{r}_\ell} \left(f_{\theta,\ell} c_{0,\ell} + \dot{f}_{\theta,\ell} c_{1,\ell} + \ddot{f}_{\theta,\ell} c_{2,\ell} \right) - d_{3,\ell} T_\ell^2 - \frac{d_{4,\ell} T_\ell^3}{3} \quad (C13)$$

Equations (36) and (37) are used as in the text to estimate the final stage cutoff time, with

$$\Delta h = h(T) - h_N(0)$$

The cutoff times of the first $N - 1$ stages are assumed fixed and equal to their nominal values.

APPENDIX D

APPROXIMATE MIDCOURSE VELOCITY REQUIREMENTS

The midcourse Δv required to correct for injection errors is approximately equal to the uncorrected miss at the moon divided by the time to impact after the correction is made

$$\Delta v_m \sim \frac{M}{T_m} \quad (D1)$$

where M is the miss at the incoming asymptote to the moon. Equation (D1) is valid because the trajectory between midcourse and the moon is nearly a straight line (all gravity forces are small in this region).

A correction time of 20 hours after injection is assumed, which gives T_m a value of approximately 46 hours. The following analysis will determine the miss associated with the various injection errors.

Error in Injection True Anomaly

An error in true anomaly is equivalent to a rotation of the translunar ellipse about \hat{h} by the error angle, so that

$$M = r_m |\Delta\eta| \quad (D2)$$

where r_m is the target distance (Earth-to-moon radius) and $\Delta\eta$ is the error in true anomaly.

Error in Perigee Radius

The energy and perigee radius can be expressed in terms of the orbital elements

$$r_p = \frac{p}{1 + e} \quad (D3)$$

$$E = \frac{\mu}{2p} (e^2 - 1) \quad (D4)$$

and the differentials are

$$dE = -\frac{\mu}{2p^2}(e^2 - 1)dp + \frac{\mu e}{p}de \quad (D5)$$

$$dr_p = \frac{(1+e)dp - pde}{(1+e)^2} \quad (D6)$$

At constant energy, equations (D5) and (D6) give

$$dp = 2e dr_p \quad (D7)$$

$$de = \frac{(e^2 - 1)}{p} dr_p \quad (D8)$$

The target true anomaly can be obtained from

$$\cos \eta_m = \frac{\frac{p}{r_m} - 1}{e} \quad (D9)$$

so that the equivalent error in true anomaly is

$$d\eta_m = \frac{\left(\frac{p}{r_m} - 1\right)de}{e^2 \sin \eta_m} - \frac{dp}{r_m e \sin \eta_m} \quad (D10)$$

In terms of dr_p ,

$$d\eta_m = -\frac{dr_p}{r_m e^2 \sin \eta_m} \left[\frac{r_m}{p}(e^2 - 1) + e^2 + 1 \right] \quad (D11)$$

and the miss at the moon is

$$M = \left| \frac{-\Delta r_p}{e^2 \sin \eta_m} \left[\frac{r_m}{p}(e^2 - 1) + e^2 + 1 \right] \right| \quad (D12)$$

Error in Injection Velocity

At constant perigee radius, equations (D5) and (D6) give

$$de = \frac{2p \, dE}{\mu(e + 1)} \quad (D13)$$

$$dp = \frac{2p^2 \, dE}{\mu(e + 1)^2} \quad (D14)$$

Using equation (D10) results in

$$d\eta_m = - \frac{2p \, dE}{\mu e(e + 1) \sin \eta_m} \left[\frac{p}{r_m(1 + e)} + \frac{\left(1 - \frac{p}{r_m}\right)}{e} \right] \quad (D15)$$

Energy is related to velocity and radius by

$$E = \frac{v^2}{2} - \frac{\mu}{r} \quad (D16)$$

At constant radius,

$$dE = v \, dv \quad (D17)$$

and the miss at the moon is

$$M = \left| \frac{-2pr_m v \, \Delta v}{\mu e(e + 1) \sin \eta_m} \left[\frac{p}{r_m(1 + e)} + \frac{\left(1 - \frac{p}{r_m}\right)}{e} \right] \right| \quad (D18)$$

Error in Yaw Velocity

Yaw velocity is defined as

$$v_h = (\hat{r} \times \vec{v}) \cdot \hat{R}_m = v_\theta (\hat{h} \cdot \hat{R}_m) \quad (D19)$$

An error in yaw velocity implies that the injection plane does not contain the target, and the corresponding miss is given by

$$M = r_m (\hat{h} \cdot \hat{R}_m) = \frac{r_m v_h}{v_\theta} \quad (D20)$$

Numerical Sensitivities

The following numerical values are assumed for the calculation of the numerical sensitivity coefficients:

Time to impact, T_m , sec	1.6×10^5
Target distance, r_m , ft	1.3×10^9
Eccentricity, e	0.986
Target true anomaly, η_m , deg	170
Semilatus rectum, p , ft	4.26×10^7
Velocity, v , ft/sec	3.6×10^4
Central body force constant, μ , ft ³ /sec ²	1.41×10^{16}
Circumferential velocity, v_θ , ft/sec	3.6×10^4

These values and equations (D1), (D2), (D12), (D18), and (D19), are used to obtain the following sensitivity coefficients:

Injection error	Midcourse Δv
True anomaly	137 (ft/sec)/deg
Perigee radius	0.241 (ft/sec)/n. mi.
Velocity	5.21 (ft/sec)/(ft/sec)
Yaw velocity	0.218 (ft/sec)/(ft/sec)

REFERENCES

1. Sarture, Charles W. : Rocket Vehicle Guidance. Inertial Guidance, George R. Pitman, ed., John Wiley & Sons, Inc., 1962, pp. 226-271.
2. Moore, F. B.; and Brooks, Melvin: Saturn Ascending Phase Guidance and Control Techniques. Preprint 2458-62, ARS, July 1962.
3. MacPherson, D. : An Explicit Method of Guiding a Vehicle from an Arbitrary Initial Position and Velocity to a Prescribed Orbit. TDR-594-(1565-01) TN-1 (DDC No. AD 265 538), Aerospace Corp., Feb. 1961.
4. Cherry, George W. : A General, Explicit, Optimizing Guidance Law for Rocket-Propelled Spaceflight. Paper 64-638, Am. Inst. Aeron. and Astronaut., Aug. 1964.
5. Teren, Fred; and Spurlock, Omer F. : Payload Optimization of Multistage Launch Vehicles. NASA TN D-3191, 1966.
6. Hildebrand, Frances B. : Methods of Applied Mathematics. Prentice-Hall, Inc., 1952.